7. Transport of Cosmic Radiation

The theory of electromagnetic radiation was first derived by James Clerk Maxwell in 1873. He showed that both magnetic and electric fields propagate in space and the velocity of propagation, from purely magnetic and electrical measurements, was very nearly 3×10^8 m/s. Within the limits of experimental error, this was equal to the velocity of propagation of light. Within fifteen years of Maxwell's discovery, Heinrich Hertz succeeded in producing electromagnetic radiation at microwave frequencies by installing a spark gap (an oscillating high-potential arc discharge across two conductors separated by a short gap) at the center of a parabolic metal mirror. While the induction field was significant in Hertz's measurements (1.5 m transmitter-receiver separations), Gugliemo Marconi succeeded in demonstrating true electromagnetic energy transport, first at separations of 9 meters, then 275 meters, then 3 kilometers, and then, in 1901, across the English Channel. Finally, in 1901, Marconi's transmissions bridged the Atlantic Ocean—a distance of 3,200 kilometers.

Like radiation at optical wavelengths, that can be decomposed into a spectrum of constituent components (reds to violets) by a prism or grating, radiation at other wavelengths is also resolvable into a spectrum, another discovery by Hertz who showed that electromagnetic waves possessed all the properties of light waves—they could be reflected, refracted, focused by a lens, and polarized.

The electromagnetic spectrum corresponds to waves of various frequencies and wavelengths, related by the equation $\lambda f=c$, where $c = 3\times10^8$ m/s is the free space velocity of light. In principle, it was found that knowledge of the radiation pattern recorded by an antenna system, and the distribution of the radiation in a frequency spectrum, could give precise information about the distant source of the radiation—its location, size, mechanism, energy, etc.

However, a complication arises when the propagation medium is no longer free space, but instead is *plasma*. The plasma may be dilute—such as the interstellar or intergalactic medium (Chapter 1), or it may be dense—for example, pinched plasma filaments that may even be the source of the radiation (Section 6.5). In both cases the properties of the radiation are altered, in the dilute case over long propagation distances and in the dense case over short propagation distances.[1]

The first complication results from a modification of the wavelength-frequency relation, $\lambda f=c/n$, where n is the refractive index of the plasma (Appendix B). Since n depends on the wave frequency, magnetic field strength and orientation, plasma temperature, plasma constituency, and collision frequency, these parameters must be taken into account when an attempt is made to unfold the nature of the distant sources such as those responsible for the spectrum shown in Figure 1.24. Additionally, linearity is no longer preserved if the wave field **E** is intense enough to modify the physical properties of the medium through which it propagates, by accelerating the plasma electrons and ions which may then collide with neutrals to heat the medium (e.g., Section 1.2.5).

This chapter starts with an outline of the mathematical description of energy transport in plasma. This is followed by a description of geometrical optics in radiation transfer—its applications and limitations. Blackbody radiation, the source function, and Kirchoff's law are covered for the case of Maxwellian particle velocity distributions, and the classical definition of radiation temperature is given. The absorption of radiation by plasma filaments, the large-scale random magnetic field approximation, and the generalization of radiation transport to anisotropic velocity distributions, finish the chapter.

7.1 Energy Transport in Plasma

A power-energy conservation relationship may be developed by expanding the divergence of the vector product $\mathbf{E} \times \mathbf{H}$, and using the Maxwell–Hertz–Heaviside curl equations (1.1) and (1.2) to obtain

$$\nabla \cdot (\mathbf{E} \times \mathbf{H}) = -\mathbf{E} \cdot \left(\mathbf{j} + \frac{\partial \mathbf{D}}{\partial t}\right) + \mathbf{H} \cdot \left(-\frac{\partial \mathbf{B}}{\partial t}\right)$$

$$= -\mathbf{E} \cdot \mathbf{j} - \frac{1}{2}\frac{\partial}{\partial t}\left(\varepsilon E^2 + \mu H^2\right) \tag{7.1}$$

Equation (7.1) is in the form of a conservation theorem and can be recast in the form

$$\nabla \cdot \mathbf{S} + \frac{\partial}{\partial t}\left(w_{\mathbf{E}\cdot\mathbf{j}} + w_E + w_B\right) = 0 \tag{7.2}$$

where

$\mathbf{S} = \mathbf{E} \times \mathbf{H}$ is the Poynting vector,

$w_{\mathbf{E}\cdot\mathbf{j}} = \int \mathbf{E} \cdot \mathbf{j}\, dt$ is the particle energy density in the fluid approximation,

$w_E = \frac{1}{2}\varepsilon E^2$ is the electric field energy density, and

$w_B = \frac{1}{2}\mu H^2$ is the magnetic field energy density.

By applying the divergence theorem to Eq.(7.2), it is seen that the outward flux of the vector S from a volume V is accounted for by a time rate of change within that volume of the electromagnetic to mechanical energy conversion term plus the electromagnetic field energy density $w_E + w_B$

$$\oint_s \mathbf{S} \cdot \mathbf{ds} = -\frac{\partial}{\partial t}\int_V \left(w_{\mathbf{E}\cdot\mathbf{j}} + w_E + w_B\right) dV \tag{7.3}$$

Although Eq.(7.2) is rigorous at every instant of time, our interest will only be in the averaged quantities. Following a procedure outlined by Bekefi [1966, p. 10] utilizing the time and space Fourier transforms of Eqs.(1.1)–(1.4), we obtain

$$\mathbf{k_i} \cdot [\overline{\mathbf{S}} + \overline{\mathbf{T}}] = \omega_i \left(\overline{w_B} + \overline{w_{E+p}}\right) + \overline{p_{E \cdot j}} \tag{7.4}$$

where $\mathbf{k_i}$ and ω_i are the imaginary components of

$$\mathbf{k} = \mathbf{k_r} + i\,\mathbf{k_i} \tag{7.5}$$

$$\omega = \omega_r + i\,\omega_i \tag{7.6}$$

and

$$\overline{\mathbf{S}} = \frac{1}{2}\mathrm{Re}\left(\mathbf{E} \times \mathbf{H}^*\right) \quad \text{is the time-averaged flux,} \tag{7.7a}$$

$$\overline{\mathbf{T}} = -\frac{1}{4}\varepsilon_0\,\mathbf{E}^* \cdot \frac{\partial \omega \mathbf{K}}{\partial \mathbf{k}} \cdot \mathbf{E} \quad \text{is the nonelectromagnetic energy flux of particles flowing coherently with wave,} \tag{7.7b}$$

$$\overline{w_B} = \frac{1}{4}\mu_0 |\mathbf{H}|^2 \quad \text{is the time-averaged magnetic energy density,} \tag{7.7c}$$

$$\overline{w_{E+p}} = \frac{1}{4}\varepsilon_0\,\mathbf{E}^* \cdot \frac{\partial \omega \mathbf{K}}{\partial \omega} \cdot \mathbf{E} \quad \text{is the time-averaged electric energy density plus kinetic energy of particles coherent with wave, and} \tag{7.7d}$$

$$\overline{p_{\mathbf{E} \cdot \mathbf{j}}} = \frac{1}{4}\varepsilon_0\,\mathbf{E}^* \cdot (\omega_r \mathbf{K_a}) \cdot \mathbf{E} \quad \text{is the time-averaged rate of power absorption.} \tag{7.7e}$$

The time-averaged Poynting vector $\overline{\mathbf{S}}$ represents the flux of electromagnetic energy. The quantity $\overline{\mathbf{T}}$ is the nonelectromagnetic energy flux due to the coherent motion of the charge carriers. In a cold plasma, where the charge carriers oscillate about fixed positions, $\overline{\mathbf{T}} = 0$. In a hot plasma, bodily transport of density, velocity, and energy fluctuations by the free-streaming particles lead to finite values for $\overline{\mathbf{T}}$.

The dissipation of energy from the wave enters through the anti-Hermitian part of the equivalent dielectric tensor $\mathbf{K_a} = (\mathbf{K} - \mathbf{K}^*)/2i$. When the medium is not time-dispersive, $\overline{w_{E+p}}$ takes on a more familiar form $\overline{w_{E+p}} = \frac{1}{4}\varepsilon_0\,\mathbf{E}^* \cdot \mathbf{K} \cdot \mathbf{E}$.

Example 7.1 Total energy density of a transverse electromagnetic wave propagating in an isotropic medium. From Eq.(B.2), since $\mathbf{B}_0 = 0$, all diagonal tensor elements reduce to $K = P = 1 - \omega_p^2/\omega^2$ and Eq.(7.7d) is

$$\overline{w_{E+p}} = \frac{1}{4}\varepsilon_0 |\mathbf{E}|^2 \left(1 + \omega_p^2/\omega^2\right) \tag{7.8}$$

Since $\mathbf{H} = \sqrt{\varepsilon_0/\mu_0}\,\mathbf{n} \times \mathbf{E}$, where $\mathbf{n}$ is given by Eq.(B.7) and $n^2 = P$ Eq.(B.11),

$$\overline{w_B} = \frac{1}{4}\varepsilon_0 |\mathbf{E}|^2 \left(1 - \omega_p^2 / \omega^2\right)$$

The total energy density is therefore

$$\overline{w_B} + \overline{w_{E+p}} = \frac{1}{2}\varepsilon_0 |\mathbf{E}|^2 \tag{7.9}$$

Example 7.2 Total energy density of a longitudinal wave in warm magnetized plasma near the second electron cyclotron harmonic. A transverse electromagnetic wave $\mathbf{E} = \mathbf{E}^{\text{inc}} e^{i(\mathbf{k}\cdot\mathbf{r} - \omega t)}$ is incident on a warm magnetized plasma slab (Figure 7.1). The propagation vector is $\mathbf{k} = \hat{\mathbf{x}}\, k_x + \hat{\mathbf{y}}\, k_y$, and $k / k_y = \sin \xi_i$, where ξ_i is the angle of incidence, and the plasma extends in the x direction. Since the electric field of the longitudinal wave is predominantly along its direction of propagation, it follows from a simple geometrical consideration that in the plasma

$$E_x^L = -\frac{c}{\omega \sin \xi_i} \frac{k_x}{} E_y^L \tag{7.10}$$

so that $|E_x^L| >> |E_y^L|$. Neglecting E_y^L, Eq.(7.7b) can be written

$$\overline{T_x} = -(\omega \varepsilon_0 / 4)\left(\partial K_{xx} / \partial k_x\right) |E_x^L|^2 \tag{7.11}$$

The element K_{xx} of the dielectric constant in warm magnetized plasma is [Peratt and Kuehl 1972]

$$K_{xx} = 1 - \frac{\omega_p^2}{\omega^2 - \omega_c^2} + \frac{c^2 k_x^2}{\omega^2}\left(\frac{\omega_p^2}{\omega^2 - \omega_c^2}\right)\left(\frac{\omega^2}{4\,\omega_c^2 - \omega^2}\right)\frac{3\,\overline{v_x^2}}{c^2} \tag{7.12}$$

Differentiating Eq.(7.12) and inserting in Eq.(7.11) gives the final result

$$\overline{T_x} = +\frac{1}{2}\sqrt{\frac{\varepsilon_0}{\mu_0}}\,\frac{c\,k_x}{\omega}\left(\frac{\omega_p^2}{\omega^2 - \omega_c^2}\right)\left(\frac{\omega^2}{4\,\omega_c^2 - \omega^2}\right)\frac{3\,\overline{v_x^2}}{c^2} \tag{7.13}$$

where the sign of Eq.(7.13) has been reversed since the phase velocity is in the opposite direction from that assumed in the derivation of Eq.(7.11).

7.1.1 Group Velocity

The velocity at which energy in the wave propagates, the group velocity, is defined as

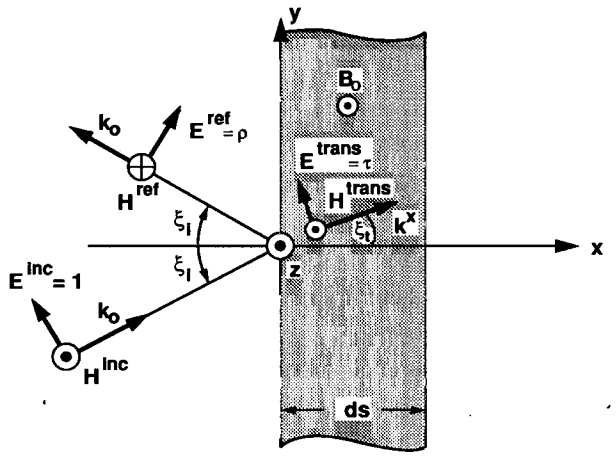

Figure 7.1. Incident, reflected, and transmitted wave vectors for a transverse electromagnetic wave obliquely incident upon a magnetized plasma.

$$v_g = \frac{\text{total time–averaged flux}}{\text{time–averaged energy density}} \tag{7.14}$$

or, from Eq.(7.7),

$$\mathbf{v_g} = \frac{\partial \omega}{\partial \mathbf{k}} = \frac{\overline{\mathbf{S}} + \overline{\mathbf{T}}}{\overline{w_B} + \overline{w_{E+p}}} \tag{7.15}$$

where

$$\frac{\partial \omega}{\partial \mathbf{k}} = \hat{\mathbf{x}} \frac{\partial \omega}{\partial k_x} + \hat{\mathbf{y}} \frac{\partial \omega}{\partial k_y} + \hat{\mathbf{z}} \frac{\partial \omega}{\partial k_z} \tag{7.16}$$

The group velocity vector $\mathbf{v}_g$ associated with the wave has a magnitude v_g and a direction given by the angles ξ and η (Figure 7.2). In spherical coordinates

$$\omega = \omega(k, \theta, \phi) \tag{7.17}$$

and Eq.(7.16) is

$$\frac{\partial \omega}{\partial \mathbf{k}} = \hat{\mathbf{k}} \frac{\partial \omega}{\partial k} + \hat{\boldsymbol{\theta}} \frac{1}{k} \frac{\partial \omega}{\partial \theta} + \hat{\boldsymbol{\phi}} \frac{1}{k \sin \theta} \frac{\partial \omega}{\partial \phi}$$

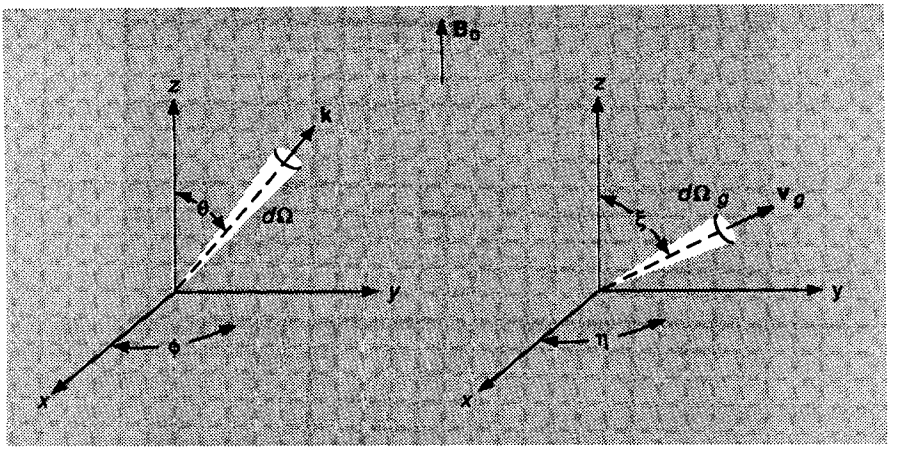

Figure 7.2. Coordinate system showing the propagation vector **k** and the associated group-velocity vector $\mathbf{v}_g$.

$$= \hat{\mathbf{k}}\, v_{gk} + \hat{\boldsymbol{\theta}}\, v_{g\theta} + \hat{\boldsymbol{\phi}}\, v_{g\phi} \tag{7.18}$$

and

$$v_{gk} = \left(\frac{\partial k}{\partial \omega}\right)^{-1}$$

$$v_{g\theta} = \frac{\partial k}{\partial \theta}\left(\frac{\partial k}{\partial \omega}\right)^{-1} \tag{7.19}$$

$$v_{g\phi} = \frac{1}{k \sin\theta}\frac{\partial k}{\partial \phi}\left(\frac{\partial k}{\partial \omega}\right)^{-1}$$

The transformations Eq.(7.19) can be simplified if an axis of symmetry $\mathbf{B}_0 = \hat{\mathbf{z}}\, B_0$ is chosen. Thus, $\partial k / \partial \phi = 0$ and

$$v_{gk} = v_g \cos(\theta - \xi)$$

$$v_{g\theta} = -v_g \sin(\theta - \xi) \tag{7.20}$$

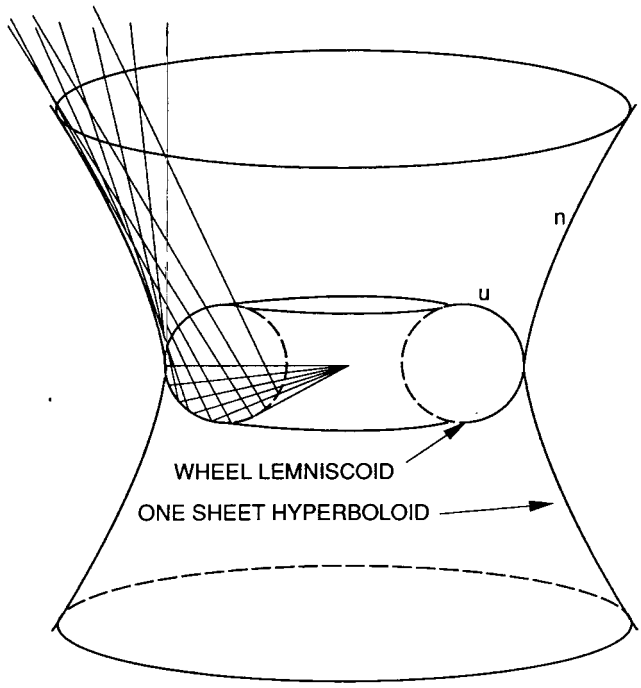

Figure 7.3. Wheel lemniscoidal normal surface and partial construction of its one sheet hyperboloidal ray surface. These shapes are representative of the compressional Alfvén wave.

$$v_{g\phi} = 0$$

From Eqs.(7.19) and (7.20)

$$\tan(\theta - \xi) = -\frac{v_{g\theta}}{v_{gk}} = \frac{1}{k}\left(\frac{\partial k}{\partial \theta}\right)_{\omega} \tag{7.21}$$

where $(\theta - \xi)$ is the angle between the direction of wave propagation **k** and the direction of energy propagation $\mathbf{v_g}$ / v_g . The differentiation of k in Eq.(7.21) is done at fixed frequency ω.

Consider, for example, a wheel lemniscoid wave-normal surface (which is representative of the compressional Alfvén wave) as shown in Figure 7.3. One may use wave-normal surfaces to find the direction of $\mathbf{v_g}$. Let the origin represent an instantaneous constructive interference maximum for a group of waves which are of the same frequency but which differ slightly in direction. At a later unit time, the wave fronts which had passed through the origin will lie on the surfaces which are perpendicular to and which contain the tip of the ω/**k** radius vector. The new point of constructive interference occurs where these wavefronts again coincide. The coinciding wave

fronts form an envelope for a second surface, which is called the ray surface when the medium is nondispersive.

For dispersive media, only the direction of the wave is given correctly by the construction of Figure 7.3. One must then consider the constructive interference of waves not only with different directions, but also with different frequencies, and the length of the $\mathbf{v}_g$ vector is changed acordingly.

Example 7.3 Whistler mode propagation through the ionosphere. A famous example of group velocity relations in anisotropic dispersive plasma is furnished by the whistler mode. Whistlers, which were first reported in 1919 by H. Barkhausen, are electromagnetic disturbances initiated by lightning discharges in the upper atmosphere, particularly the electromagnetic radiation with frequencies of 300 Hz to 30 KHz. The waves cannot be heard directly but are converted into audible sound waves of the same frequency by an audioamplifier. They are propagated from one hemisphere to another in the ionosphere and follow the earth's dipole magnetic field lines. In propagation through the ionosphere the group velocity is proportional to the square-root of the frequency so that the received signal is a descending tone lasting a few seconds.

We write Eq.(B.10) in the form

$$n^2 = 1 - \frac{2(A - B + C)}{2A - B \pm \sqrt{B^2 - 4AC}} \tag{7.22}$$

Using the "quasi-longitudinal" approximation

$$\omega_p^2 \sin^4 \theta << 4\,\omega^2 \left(1 - \omega_p^2 / \omega^2\right)^2 \cos^2 \theta \tag{7.23}$$

in addition to the approximation

$$\omega_p^2 \sin^2 \theta << \left| 2\,\omega^2 \left(1 - \omega_p^2 / \omega^2\right) \right| \tag{7.24}$$

we arrive at the quasi-longitudinal right-hand index of refraction equation

$$n^2 = 1 - \frac{\omega_p^2 / \omega}{\omega - \omega_b \cos \theta} \tag{7.25}$$

In his analysis of this mode, Storey [1953] simplified Eq.(7.25) to obtain the approximate form

$$n^2 = 1 - \frac{\omega_p^2}{\omega\ \omega_b \cos \theta} \tag{7.26}$$

which is valid where $|\omega_b \cos \theta| >> |\omega|$ and when $n^2 >> 1$. Thus, the frequency and group velocity are

$$\omega = \frac{c^2 k^2 \omega_b}{\omega_p^2} \cos\theta \tag{7.26a}$$

$$\frac{\partial \omega}{\partial k} = \frac{2k\ c^2 \omega_b}{\omega_p^2} \cos\theta = \frac{2c}{\omega_p} \sqrt{\omega_b \cos\theta}\sqrt{\omega} \tag{7.26b}$$

From Eqs.(7.21) and (7.26), $\tan(\theta - \xi) = \frac{1}{2}\tan\theta$. Solving for ξ gives

$$\xi = \tan^{-1}\left(\frac{\sin\theta\cos\theta}{1+\cos^2\theta}\right) \tag{7.27}$$

The maximum possible value of ξ is found by differentiating Eq.(7.27) with respect to θ and setting it equal to zero. After some manipulation we find that

$$\xi_{max} = \tan^{-1} 2^{-3/2} = 19^\circ\ 29'$$

where ξ is the angle between the ray direction and the earth's dipole magnetic field lines. This angular limitation on the group-velocity direction accounts for the tendency of whistlers to follow the lines of force of the earth's magnetic field. The frequency dependence of the group velocity accounts for the whistler's characteristic descending tone since the higher frequency components of the disturbance arrive first.

An example of a 500 Hz whistler-mode ray path obtained using a ray tracing program is shown in Figure 7.4 [Kimura 1966].

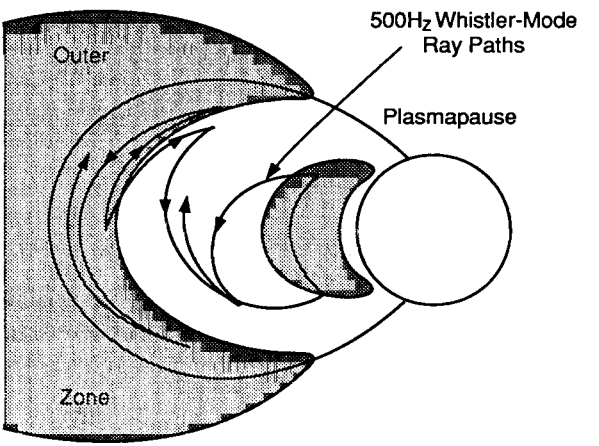

Figure 7.4. Example of 500 Hz whistler-mode ray paths, obtained from a ray tracing program, that illustrates how wave energy generated in the outer region of the plasmasphere can propagate across magnetic field lines so as to fill the plasmasphere with waves.

7.1.2 Time Rate of Decay of Wave Oscillations

The time-averaged rate of power absorption divided by the time-averaged electromagnetic energy density in the waves gives the time rate of decay of the oscillations, that is,

$$\tau = \left[\frac{\overline{p_{\mathbf{E}} \cdot \mathbf{j}}}{\overline{w_E} + \overline{w_B}} \right]^{-1} \quad \text{s} \tag{7.28}$$

An alternate way of expressing the time rate of decay and spatial absorption of a plane wave is through the complex values of ω [Eq.(7.5)] and $\mathbf{k}$ [Eq.(7.6)]. The relaxation time for the oscillations is $(-\omega_i)^{-1}$; therefore the relaxation time for energy is

$$\tau = (-2\,\omega_i)^{-1} \quad \text{s} \tag{7.29}$$

Likewise, the spatial damping is $(\mathbf{k}_i)^{-1}$; therefore the absorption is

$$\alpha_\omega = 2\,k_i \quad \text{m}^{-1} \tag{7.30}$$

However, the absorption coefficient must be corrected to include the direction of wave propagation $\mathbf{k}$ with respect to its group velocity $\partial\omega / \partial\mathbf{k}$. This correction is (Figure 7.2)

$$\alpha_\omega = 2\,k_i \cos\left(\theta - \xi\right) \quad \text{m}^{-1} \tag{7.31}$$

7.2 Applications of Geometrical Optics

Geometrical optics assumes that the medium varies slowly with position and the scale length of the variations is much longer than the wavelength of the radiation in the medium. The radiation can then be considered as being transported along bundles of curves or rays (Figure 7.5). In plasma, the various bundles may belong to the different characteristic plasma modes of propagation. Nevertheless, unlike the mode conversion processes described in Appendix B, in geometrical optics the bundles do not interact with one another.

7.2.1 Basic Principle and Limitations of Geometrical Optics

Consider for a moment a loss-free plasma ($\overline{p_{\mathbf{E}} \cdot \mathbf{j}} = 0$) under steady state conditions ($\omega = 0$, $\nabla \leftrightarrow i\,\mathbf{k}$) so that Eq.(7.4) may be expressed as

$$\nabla \cdot \overline{\mathbf{F}_\omega} = 0 \tag{7.32}$$

The quantity $\mathbf{F}_\omega$ is called the spectral flux and consists of both the electromagnetic flux and the flux of particles

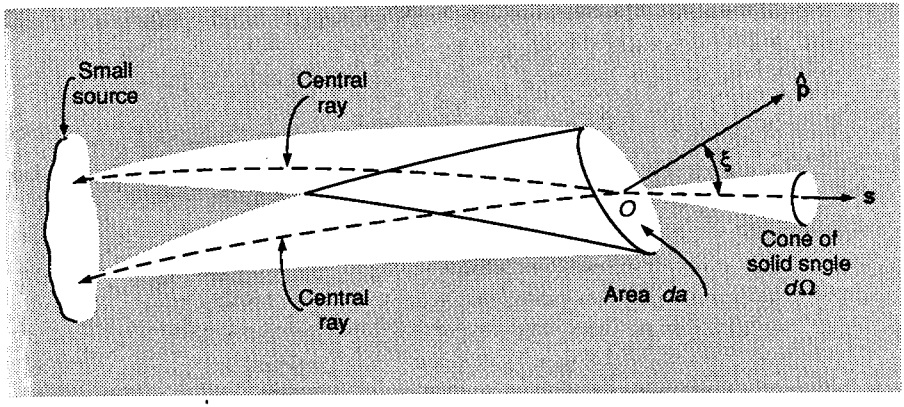

Figure 7.5. Bundles of rays emanating from a small source crossing an element of area *da*.

$$\overline{\mathbf{F}_\omega} = \overline{\mathbf{S}(\omega)} + \overline{\mathbf{T}(\omega)} \tag{7.33}$$

Since Eq.(7.32) is valid for each possible mode supported by the plasma separately of any other mode, the flux $\overline{\mathbf{F}_\omega}$ is the total flux for a single mode.

The problem of flux flow is handled as follows. Let *da* be a small area in plasma whose outward normal is along $\mathbf{B}_0$. Each element of the source sends through *da* a tube of rays, and the central rays of the tubes fill a cone of solid angle $d\Omega$. For a sufficiently small cone angle the fluxes from the individual elements travel essentially in the same direction. If the sources are assumed to radiate incoherently with respect to one another, the total flux is the scalar sum of the individual fluxes. The magnitude of this flux is then

$$d\mathbf{F}_\omega \cdot \hat{\mathbf{z}} = dF_\omega \cos\xi = I_\omega(s) \cos\xi \, d\Omega \tag{7.34}$$

where I_ω is a constant of proportionality. The time-averaged power P_ω in the spectral range $d\omega$, crossing the elementary area *da* and confined to the cone $d\Omega$ is

$$dP_\omega = I_\omega(s) \cos\xi \, d\Omega \, da \, d\omega \quad \text{W m}^{-2} \text{ ster}^{-1} \tag{7.35}$$

The scalar quantity I_ω is known as the specific intensity of radiation or, simply, the intensity. If I_ω at a point is independent of direction, the radiation is isotropic.

To obtain the total flux crossing unit area da (Figure 7.6), Eq.(7.34) must be integrated over 4π steradians:

$$F_\omega = \int_{0<\xi<\pi} I_\omega(s) \cos\xi \, d\Omega \tag{7.36}$$

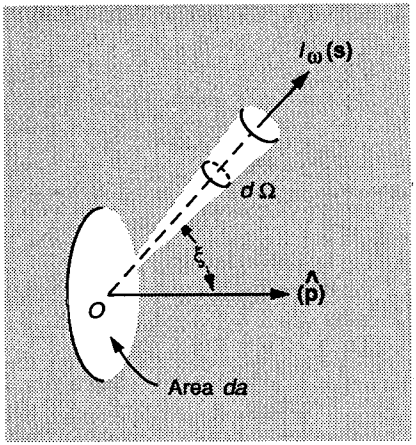

Figure 7.6. Vector diagram for radiation flowing across a small area da.

In radio astronomy the measurement of the flux takes place at a large distance from the radiating body and, since the body subtends a sufficiently small solid angle at the position of the observer, Eq.(7.36) can be approximated by

$$F_\omega = \int_{0<\xi<\pi} I_\omega(s)\, d\Omega$$

Consider an infintesimal volume element of the plasma in the form of a pillbox as shown in Figure 7.7. A pencil with radiation intensity I_ω and solid angle $d\Omega_1$ enters one face at an angle ξ_1 to the normal $\hat{\mathbf{z}}$. The radiation in the outgoing beam of intensity $I_\omega + dI_\omega$ leaves within a solid angle $d\Omega_2$. If the plasma is simple and slightly inhomogeneous, it causes a bending of the rays, so that $\xi_1 \neq \xi_2$. If the medium is also loss-free then, in accordance with Eq.(7.35)

$$(I_\omega + dI_\omega)\cos\xi_2 d\Omega_2\, da\, d\omega - I_\omega \cos\xi_1 d\Omega_1\, da\, d\omega = 0 \tag{7.37}$$

which is the energy conservation equation for radiation propagating along a bundle of rays. For a simple plasma, Snell's law of refraction may be employed which states

$$n \sin\xi = \text{constant along the ray} \tag{7.38}$$

where n is the real part of the refractive index Eq.(B.7). We then find that

$$n^2 da \cos\xi\, d\Omega = \text{constant} \tag{7.39}$$

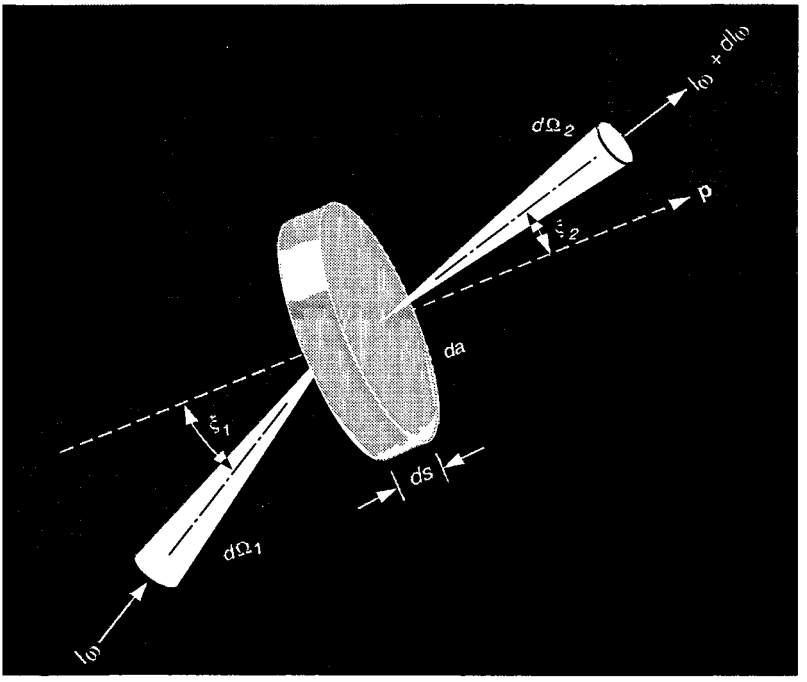

Figure 7.7. Radiation entering a small volume of plasma and leaving it after having suffered a small amount of refraction due to a difference in refractive indices on the two sides of the elementary pillbox.

and from Eq.(7.37) that

$$I_\omega / n^2 = \text{constant along the ray} \tag{7.40}$$

In magnetized, anisotropic, and inhomogeneous plasma, the rigourous solution of the ray trajectory problem is beset with the same basic difficulty of geometrical optics: the wavelength must be short compared to the distance over which the refractive index changes appreciably. This requirement is often violated in cosmic plasma, where transistion regions define abrupt changes in plasma density, temperature, and magnetic field strength. In addition, plasma wave theory shows that the refractive index may change rapidly even though the plasma density or magnetic field changes gradually (Figure B.1).

Example 7.4 Absence of a Brewster's Angle in anisotropic plasma. Referring to Figure 7.1, where $\mathbf{E} \perp \mathbf{B}_0$, the sum of the incident and reflected waves at the plasma boundary may be written as

$$E_y = (1 + \rho) \cos \xi_i \tag{7.41}$$

$$\sqrt{\frac{\mu_0}{\varepsilon_0}}\, H_z = (1-\rho) \tag{7.42}$$

Within the plasma half-space, $\mathbf{E} \perp \mathbf{B}_0$, so that the field is extraordinary and consists of components both perpendicular and parallel to $\mathbf{k}$

$$E_y^{(X)} = E_\perp \cos \xi_t + E_{\parallel} \sin \xi_t \tag{7.43}$$

where ξ_t is given by Snell's law $\sin \xi_i = n^{(X)} \sin \xi_t$. A relationship between $E_\perp$ and $E_{\parallel}$ may be obtained by briefly considering the case $\xi_i = 0$. In this case $E_x = E_{\parallel}$ and $E_y = E_\perp$. From the vector wave equation Eq.(B.9), $S\, E_x - i\, D\, E_y = 0$, or

$$E_{\parallel} = -i \frac{\omega_b}{\omega} \frac{\omega_p^2/\left(\omega_b^2 - \omega^2\right)}{\omega_p^2/\left(\omega_b^2 - \omega^2\right) - 1} E_\perp \tag{7.44}$$

Since Eq.(7.44) is independent of coordinate rotation, it is valid at angle ξ_t. Substituting Eq.(7.44) into Eq.(7.43)

$$E_y^{(X)} = E_\perp \left[\cos \xi_t - i \frac{\omega_b}{\omega} \frac{\omega_p^2/\left(\omega_b^2 - \omega^2\right)}{\omega_p^2/\left(\omega_b^2 - \omega^2\right) - 1} \sin \xi_t \right] e^{i \left[(n^X)^2 - \sin^2 \xi_i\right]^{1/2} \frac{c}{\omega} x} \tag{7.45}$$

$$H_z^{(X)} = n^X E_\perp \, e^{i \left[(n^X)^2 - \sin^2 \xi_i\right]^{1/2} \frac{c}{\omega} x} \tag{7.46}$$

The two unknowns ρ and $\tau = E_\perp$ are obtained by matching Eq.(7.41) and Eq.(7.42) to Eq.(7.45) and Eq.(7.46) at the vacuum-plasma interface. We obtain

$$\rho = \frac{\cos(\xi_t + \xi_i) \sin(\xi_t - \xi_i) + i(\omega/\omega_b)\left[a/(a-1)\right] \sin^2 \xi_t}{\sin(\xi_t + \xi_i) \cos(\xi_t - \xi_i) + i(\omega/\omega_b)\left[a/(a-1)\right] \sin^2 \xi_t} \tag{7.47}$$

$$\tau = \frac{2 \cos \xi_i \sin \xi_t}{\sin(\xi_t + \xi_i) \cos(\xi_t - \xi_i) + i(\omega/\omega_b)\left[a/(a-1)\right] \sin^2 \xi_t} \tag{7.48}$$

where $a = \omega_p^2/\left(\omega^2 - \omega_b^2\right)$. When $\omega_b = 0$, Eq.(7.47) reduces to the well-known Fresnel equation for reflection from a dielectric with E in the plane of incidence [Slater and Frank 1947]. For $\omega_b = 0$, we may therefore have $\rho = 0$ at the "Brewster angle," but if $\omega_b \neq 0$, Eq.(7.47) shows that ρ never vanishes, so there is no "Brewster angle" for anisotropic plasma.

Example 7.5 Absorption due to collisions. Collisional effects such as wave damping caused by particle interactions can play an important role in the propagation of electromagnetic waves through cosmic plasma. For example, collisions are particularly important for longitudinal wave

propagation because of their slow group velocity. Collisional processes become important for the propagation of an extraordinary wave near a resonance.

The effect of collisions can be included in the formulation of Example 7.4 with the frequency replacement Eq.(7.6) (this is usually carried out in the derivation of the current density **j**). The quantity ω_i is considered a "collisional frequency" [Kuehl, O'Brien, and Stewart 1970] whose magnitude is determined by the type of particles in collision. With this substitution, the absorption is

$$\alpha_\omega = 1 - |\rho|^2 - |\tau|^2 \tag{7.49}$$

None of the wave conversion, wave matching, or collisional damping carried out in Examples 7.4 and 7.5 exist in geometrical optics. Nevertheless, in spite of the inadequacies of the procedure, especially at longer wavelengths, we shall continue to confine ourselves to applications of geometrical optics.

7.2.2 Equation of Transfer

In the presence of dissipation, Eq.(7.32) takes the form

$$\nabla \cdot \overline{\mathbf{F}_\omega} = \overline{(p_{\mathbf{E}} \cdot \mathbf{j})_\omega} \tag{7.50}$$

where $(p_{\mathbf{E}} \cdot \mathbf{j})_\omega$ represents the spectral density of $p_{\mathbf{E}} \cdot \mathbf{j}(t)$. The effect of dissipative processes is the appearance of absorption which, in the geometrical optics formalism, is described by

$$-\alpha_\omega \, ds \, I_\omega \cos\xi \, d\Omega \, da \, d\omega \tag{7.51}$$

The pillbox is also a source of radiation. For an emission coefficient j_ω Eq.(6.85), the power generated is

$$j_\omega \, ds \cos\xi \, d\Omega \, da \, d\omega \tag{7.52}$$

Summing Eqs.(7.51) and (7.52), placing the sum on the right-hand side of Eq.(7.37), and using Eq.(7.39), leads to the Equation of Transfer[2]

$$\boxed{n^2 \frac{d}{ds}\left(\frac{I_\omega}{n^2}\right) = -\alpha_\omega I_\omega + j_\omega} \tag{7.53}$$

All quantities of Eq.(7.53) refer to one mode of propagation and there are as many first-order differential equations like Eq.(7.53) as there are characteristic modes in the plasma.

The following are special cases where the solution to Eq.(7.53) is simple:

(1) Emission only: $\alpha_\omega = 0$

$$n^2 \frac{d}{ds}\left(\frac{I_\omega}{n^2}\right) = j_\omega, \quad \frac{I_\omega(s)}{n^2(s)} = \frac{I_\omega(s_0)}{n^2(s_0)} + \int_{s_0}^{s} \frac{j_\omega}{n^2} ds \tag{7.54}$$

(2) Absorption only: $j_\omega = 0$

$$n^2 \frac{d}{ds}\left(\frac{I_\omega}{n^2}\right) = -\alpha_\omega I_\omega, \quad \frac{I_\omega(s)}{n^2(s)} = \frac{I_\omega(s_0)}{n^2(s_0)} \exp\left\{-\int_{s_0}^{s} \alpha_\omega ds\right\} \tag{7.55}$$

(3) Thermodynamic equilibrium: For complete equilibrium of the radiation with its surroundings, the intensity is described by the Planck function at equilibrium temperature T.

$$n^2 \frac{d}{ds}\left(\frac{I_\omega}{n^2}\right) = 0, \quad \frac{I_\omega(s)}{n^2(s)} = B_0(\omega, T) \tag{7.56}$$

where $B_0(\omega, T)$ is the Planck law (Section 7.3).

In general, to solve Eq.(7.53) we define two quantities. The first

$$S_\omega = \frac{1}{n^2} \frac{j_\omega}{\alpha_\omega} \tag{7.57}$$

is known as the *ergiebigkeit* or *source function*. The second is the optical depth τ_ω

$$d\tau_\omega = -\alpha_\omega ds \tag{7.58}$$

In terms of these quantitites, Eq.(7.53) becomes

$$\boxed{\frac{d}{d\tau_\omega}\left(\frac{I_\omega}{n^2}\right) = \frac{I_\omega}{n^2} - S_\omega} \tag{7.59}$$

The solution of Eq.(7.59) is obtained by first multiplying by $e^{-\tau_\omega}$ and then partially integrating over τ_ω.

$$\int_0^{\tau_\omega(0)} e^{-\tau_\omega} \frac{dI_\omega / n^2}{d\tau} d\tau_\omega = \frac{I_\omega}{n^2} e^{-\tau_\omega}\Big|_0^{\tau_\omega(0)} + \int_0^{\tau_\omega(0)} \frac{I_\omega}{n^2} e^{-\tau_\omega} d\tau_\omega = \int_0^{\tau_\omega(0)} \left(\frac{I_\omega}{n^2} - S_\omega\right) e^{-\tau_\omega} d\tau_\omega$$

$$\frac{I_\omega}{n^2}\tau_\omega(0)\,e^{-\tau_\omega(0)} - \frac{I_\omega}{n^2}\tau_\omega(s_0)\,e^{-0} = -\int_0^{\tau_\omega(0)} S_\omega\, e^{-\tau_\omega}\, d\tau_\omega$$

or, finally,

$$\boxed{\frac{I_\omega(s)}{n^2(s)} = \frac{I_\omega(0)}{n^2(0)}\, e^{-\tau_\omega(0)} + \int_0^{\tau_\omega(0)} S_\omega\, e^{-\tau_\omega}\, d\tau_\omega} \tag{7.60}$$

Because of the definition Eq.(7.58), τ_ω decreases as s increases as shown in Figure 7.8. Thus if l is the length of the ray,

$$\boxed{\tau_\omega = -\int_l^s \alpha_\omega\, ds} \tag{7.61}$$

Equation (7.60) expresses the fact that the intensity is the sum total of the emission at all interior points, reduced by the factor $e^{-\tau_\omega}$ that allows for the absorption by the intervening plasma, to which must be added the intensity of radiation incident on the back side of the plasma, reduced by the absorption in traversing the plasma.

The emission at a given frequency has two characteristic regimes, depending on the value of the total optical depth $\tau_{\omega 0}$:

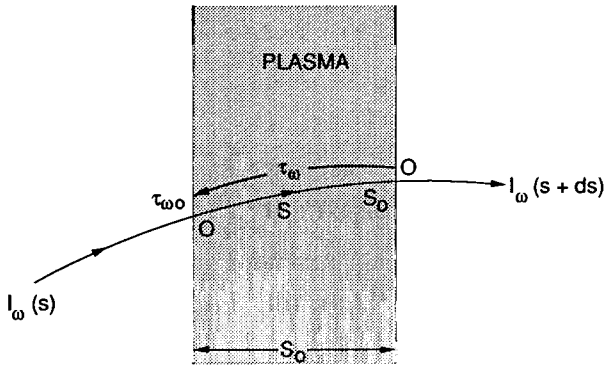

Figure 7.8. A ray passing through plasma. The optical depth τ_ω is measured from s_o, the point of emergence of the ray.

(1) When $\tau_{\omega 0} << 1$, the radiation seen by the observer suffers negligible absorption during its passage through the plasma. The plasma is said to be transparent to the radiation.

(2) When $\tau_{\omega 0} >> 1$, then $I_\omega \to n^2 S_\omega$ and the intensity depends on the refractive index and the source function. The plasma is opaque. If the plasma is isotropic and in thermal equilibrium such that $T_r = T$, where T is the true temperature of the radiators, the plasma emits as a black body (Section 7.4).

For a plasma of sufficiently large optical depth, most of the radiation seen by the external observer Eq.(7.60) comes from the outer layer of thickness $\tau_\omega \sim 1$.

7.3 Black Body Radiation

The spectral distribution of the radiation of a black body in thermodynamic equilibrium, for a single polarization, is given by the Planck formula

$$B_0(\omega, T) = \frac{\hbar \omega^3}{8 \pi^3 c^2} \frac{1}{e^{\hbar \omega / k T} - 1} \tag{7.62}$$

which is plotted for various temperatures T in Figure 7.9. On integrating Eq.(7.62) over all frequencies ω (see e.g., Reif [1965 Section A. 11]), and multiplying by 2 to include both polarizations, we obtain Stefan's law for the total brightness of a black body

$$B_0(T) = \frac{2 \pi^5 k^4 T^4}{15 c^2 h^3} = \sigma T^4 \tag{7.63}$$

where $\sigma = 5.67 \times 10^{-8}$ W m^{-2} K^{-4} is the Stefan-Boltzmann constant. The frequency at which the intensity reaches its maximum is found by solving the equation $\partial B_0(\omega, T) / \partial \omega = 0$. The final result is

$$\left(\frac{\hbar \omega}{kT}\right)_{\max} = 2.822 \tag{7.64}$$

or

$$\left(\frac{\omega}{T}\right)_{\max} = 3.69 \times 10^{11} \text{ rad s}^{-1} \text{ °K}^{-1} \tag{7.65}$$

which is known as Wien's displacement law. Approximations to Eq.(7.62) can be found in the following limiting cases.

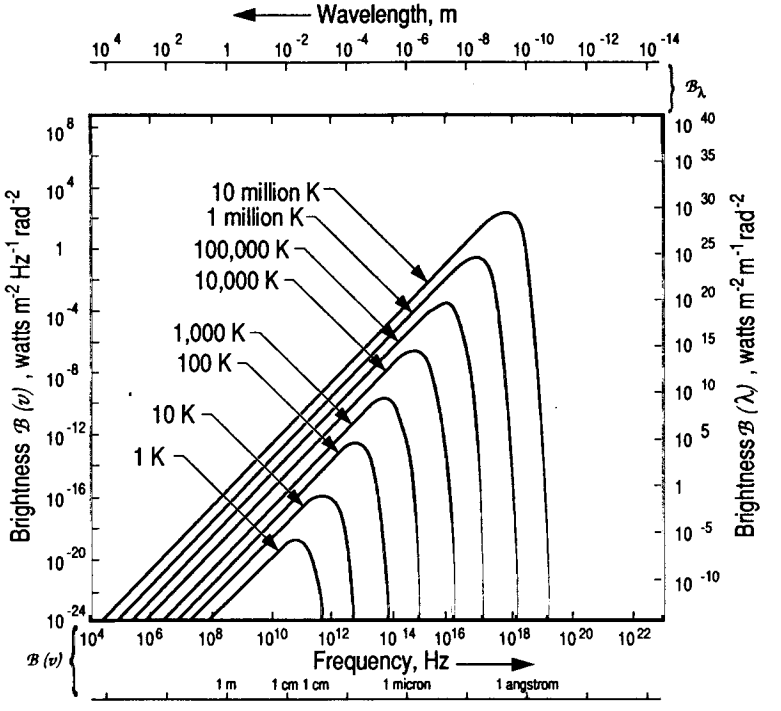

Figure 7.9. Planck-radiation-law curves at various temperatures with frequency increasing to the right (adapted from J.D. Krauss 1986).

(1) $\hbar\,\omega << kT$: Rayleigh–Jeans law (long wavelength case)

$$B_0(\omega, T) = \frac{\omega^2}{8\,\pi^3\,c^2}\,kT \tag{7.66}$$

This is the classical limit since it does not contain Planck's constant.

(2) $\hbar\,\omega >> kT$. Wien's law (short wavelength case)

$$B_0(\omega, T) = \frac{\hbar\omega^3}{8\,\pi^3\,c^2}\,e^{-\hbar\,\omega\,/\,k\,T} \tag{7.67}$$

7.4 The Source Function and Kirchoff's Law

From the theory of spontaneous and stimulated emission [Bekefi 1966], the absorption coefficient finds yet another definition:

$$\alpha_\omega = \frac{8\pi^3 c^2}{n^2 \hbar \omega^3} \int P_\omega(p') \left[f(p) - f(p') \right] d^3 p' \tag{7.68}$$

where p is the momentum corresponding to energy W - $\hbar\omega$. Substituting Eq.(7.68) and Eq.(6.85b) into Eq.(7.57), gives

$$S_\omega = \frac{1}{n^2} \frac{j_\omega}{\alpha_\omega} = \frac{\hbar \omega^3}{8\pi^3 c^2} \frac{\int P_\omega(p') f(p') d^3 p'}{\int P_\omega(p') \left[f(p) - f(p') \right] d^3 p'} \tag{7.69}$$

Equation (7.69) is a form of Kirchoff's law for anisotropic, nonthermal plasma. When the particle distribution is Maxwellian, $f(p)$ is given by Eq.(6.89) and

$$\begin{aligned} \left[f(p) - f(p') \right] &= C_p e^{-(W - \hbar\omega)/kT} - C_p e^{-W/kT} \\ &= f(p) \left(e^{\hbar\omega/kT} - 1 \right) \end{aligned} \tag{7.70}$$

Hence, Eq.(7.68) becomes

$$(\alpha_\omega)_{\text{Maxwellian}} = \frac{8\pi^3 c^2}{n^2 \hbar \omega^3} \left(e^{\hbar\omega/kT} - 1 \right) \int P_\omega(p') f(p) d^3 p' \tag{7.71}$$

or, from the definition Eq.(6.85b)

$$(\alpha_\omega)_{\text{Maxwellian}} = \frac{8\pi^3 c^2}{n^2 \hbar \omega^3} \left(e^{\hbar\omega/kT} - 1 \right) j_\omega \tag{7.72}$$

Using Eqs.(7.57) and (7.62), the source function for a Maxwellian distribution is

$$\boxed{(S_\omega)_{\text{Maxwellian}} = \frac{1}{n^2} \left(\frac{j_\omega}{\alpha_\omega} \right)_{\text{Maxwellian}} = B_0(\omega, T)} \tag{7.73}$$

Thus, when the particle distribution is Maxwellian, the source function equals the vacuum black-body intensity $B_0(\omega, T)$. The quantity T refers to the temperature of the emitting electrons; neither the energy nor the distribution function of any other species of plasma particles enters into Eq.(7.73). For example, the velocity distribution of streaming electrons or background (or collectively accelerated ions) within the plasma may be non-Maxwellian and their mean energy different from the value $3\,kT/2$.

For tenuous plasma $n \rightarrow 1$ and Eq.(7.73) reduces to what is generally considered to be the classical form of Kirchoff's law.

By analogy with vacuum black-body radiation we may write that $S_\omega = (n^2 \hbar\,\omega^3 / 8\,\pi^3 c^2)(e^{\hbar\omega/kT} - 1)^{-1}$, where the radiation temperature T_r now plays the role of the true temperature T of equilibrium radiation. Equating this to Eq.(7.69) defines T_r:

$$k\,T_r = \hbar\,\omega \left[\ln \frac{\int P_\omega(p')\, f(p)\, d^3p'}{\int P_\omega(p')\, f(p')\, d^3p'} \right]^{-1} \tag{7.74}$$

It is noted that T_r is a fictitious temperature and depends on the particle distribution, the frequency of observation, and the direction of propagation.

7.4.1 Classical Limit of the Emission, Absorption, and Source Functions

This book is primarily concerned with the classical range of frequencies $\hbar\,\omega \ll$ particle energy, and this limit is applied to the previous equations. We first consider the case in which $f(p)$ is isotropic (i.e., a function only of $p^2 = p_x^2 + p_y^2 + p_z^2$).

At our low frequencies of interest, we shall use the fact that the energy states of the particle are closely spaced. Writing that $p' = p + \Delta p$ and using Eq.(6.90) with the energy conservation equation,

$$W' - W = \hbar\,\omega \tag{7.75}$$

gives

$$\Delta p = \frac{W\,\Delta\,W}{c^2 p} = \frac{\hbar\,\omega\,W}{c^2 p}$$

We now expand $f(p') = f(p + \Delta p)$ in a Taylor series and keep only the leading terms. It follows that

$$f(p') = f(p) + \hbar\,\omega \frac{\partial f}{\partial W} \tag{7.76}$$

Substitution into Eqs.(6.85b), (7.68) and (7.69) gives the desired equations:

$$j_\omega = \int P_\omega(\mathbf{p}) f(p)\, d^3p \tag{7.77}$$

$$\alpha_\omega = -\frac{8\pi^3 c^2}{n^2 \omega^2} \int P_\omega(\mathbf{p}) \frac{\partial f(p)}{\partial W} d^3p \tag{7.78}$$

This equation was derived by Trubnikov (1958) for $n = 1$ for the study of cyclotron radiation from fusion plasmas. Often, Eqs.(7.77) and (7.78) are expressed in terms of the distribution of energy rather than through the distribution of momenta. The two are related as follows:

$$dN = f(p)\, 4\pi p^2 dp = N(W)\, dW \tag{7.79}$$

with the result that

$$j_\omega = \int P_\omega(W)\, N(W)\, dW \qquad \mathrm{J\ m^{-3}\ s^{-1}\ rad^{-1}\ ster^{-1}} \tag{7.80}$$

$$\alpha_\omega = -\frac{8\pi^3 c^2}{n^2 \omega^2} \int \left(\frac{d}{dW} \frac{N(W)}{W^2}\right) W^2 P_\omega(W)\, dW \qquad \mathrm{m^{-1}} \tag{7.81}$$

From the definitions of S_ω and T_r we also obtain from Eqs.(7.77) and (7.78)

$$k T_r = -\frac{\int P_\omega(\mathbf{p}) f(p)\, d^3p}{\int P_\omega(\mathbf{p}) \left(\partial f(p) / \partial W\right) d^3p} \tag{7.82}$$

$$S_\omega = \frac{\omega^2}{8\pi^3 c^2} k T_r \tag{7.83)}$$

When f is a Maxwellian distribution, T_r equals the electron temperature T and S_ω is the Rayleigh–Jeans limit of the Planck function.

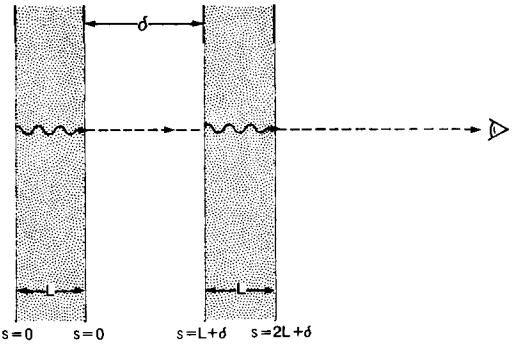

Figure 7.10. Radiation intensity seen by an observer through two successive Birkeland currents of width L and distance δ apart.

7.5 Self Absorption by Plasma Filaments

Cosmic plasma is often filamentary, caused by the electrical currents it conducts. Since these currents are the source of synchrotron radiation, it is of interest tc determine the absorption caused by the filaments themselves. The problem at hand is illustrated in Figure 7.10.

We first consider the absorption of a single filament. Applying the initial condition $I_\omega(0) = 0$ to Eq.(7.60), we obtain

$$\frac{I_\omega(s)}{n^2(s)} = S_\omega\left(1 - e^{-\tau_\omega(0)}\right) \tag{7.84}$$

Making the simplifying assumption that $n^2 \sim 1$ and using Eq.(7.58),

$$I_{\omega 1} = S_\omega\left(1 - e^{-\alpha_\omega L}\right) \tag{7.85}$$

where $I_{\omega 1}$ is the intensity of a single filament of width L. If there are now two filaments a distance δ apart the radiation intensity seen by an observer is

$$I_{\omega 2} = S_\omega\left(1 - e^{-2\alpha_\omega L}\right) \tag{7.86}$$

We have used the initial conditions for the second filament $I_{\omega 2}(s = L + \delta) = I_{\omega 1}$. Similarly, for M filaments a distance δ apart, the radiation intensity can be shown to be equal to

$$I_{\omega M} = S_\omega\left(1 - e^{-M\,\alpha_\omega L}\right) \tag{7.87}$$

Note that the radiation intensity increased for larger M because of each additional filament current source. If the plasma electrons in a current filament are in equilibrium with a Maxwellian distribution, the absorption coefficient α_ω is given by Eq.(7.78) with $n^2 = 1$. Substituting Eqs.(6.66), (6.89), and (6.92) into Eq.(7.78), the absorption coefficient at $\theta = \pi/2$ is [Trubnikov 1958]

$$\alpha_\omega = \frac{\omega_p^2}{\omega_b\, c} \sum_m \Phi_m(\omega / \omega_b, \mu) \tag{7.88}$$

The quantities $\Phi_m = \Phi_m(\omega / \omega_b, \mu)$ are defined by

$$\Phi_m = \sqrt{2\,\pi}\, \frac{\mu^{5/2}}{(\omega / \omega_b)^4}\, m^2 \sqrt{m^2 - (\omega / \omega_b)^2}\; e^{-\mu(m/(\omega/\omega_b)-1)}\, A\left[m / (\omega / \omega_b)\right] \tag{7.89}$$

where $\mu = m_0\, c^2 / k\, T$. The quantities $A_m = A_m(\gamma)$ are given by Eq.(6.80).

The optical depth for M Birkeland currents is $\tau_\omega = \alpha_\omega M L$ or

$$\tau_\omega = \left(\frac{\omega_p^2\, L\, M}{\omega_b\, c}\right) \sum_m \Phi_m \tag{7.90}$$

The spectral characteristics of the emission are contained in the function Φ. Figure 7.11 shows a plot of $\Sigma\Phi_m$ for the first one hundred harmonics as a function of ω/ω_b for $T = 30$ keV. This value is typical of the thermal temperatures in a plasma filament but is appreciably less than the energies of particles in a relativistic beam. Only the extraordinary wave is considered; the contributions from the ordinary wave are usually small.

The broadening of the individual lines is due to the relativistic change of mass. A given line contributes only to frequencies $\omega \leq m\ \omega_b$ with the highest energy electrons being responsible for the emission at the lowest frequency. The smearing of the successive harmonics produces an almost monotonically decreasing spectrum at higher frequency. For $T = 30$ keV, $m \sim 5$ is the harmonic above which smearing prevails.

To a fair approximation, the total intensity leaving the filaments is

$$I(\theta = \pi/2) \cong \int_0^{\omega^*} B_0(\omega, T)\, d\omega = \frac{\omega_b^3\, k\, T}{24\, \pi^3\, c^2} (m^*)^3 \tag{7.91}$$

where $m^* = \omega^* / \omega_t$ is the harmonic number beyond which the emission effectively ceases to be black-body. An empirical relation for m^* for mildly relativistic plasma has been derived by Trubnikov [1958]; and modified to the case of M filaments,

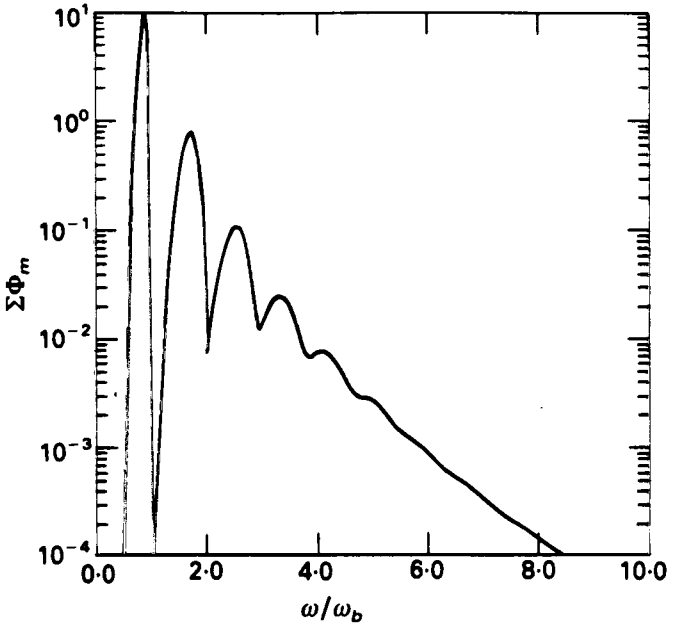

Figure 7.11. Calculated spectrum of radiation emitted by a plasma with electron temperature of 30 keV. Self-absorption effects are included.

$$(m^*)^6 = 0.57\left(\frac{20\,\omega_p^2}{3\,\omega_b\,c}\right) L\,M\,T \tag{7.92}$$

Equation (7.92) is valid under the approximation $m\,c^2 >> k\,T$

Example 7.6 Number of filaments required to produce a blackbody spectrum up to 100 GHz. Consider filaments of density $n_e = 2\times10^{-3}\,\mathrm{cm}^{-3}$, magnetic field $B_0 = 2.5\times10^{-4}\,\mathrm{G}$, temperature $T_e = 30\,\mathrm{KeV}$, and width $L = 10^{21}\,m$. From Eq.(7.92), $m^* = 1.8\times10^8$, hence $M = 3.4\times10^{31}$ filaments (Figure 7.12). This geometrical optics calculation neglects, of course, all possible reflections and resonant absorption effects.

7.6 Large-Scale, Random Magnetic Field Approximation

Magnetic fields in cosmic plasmas are generally ordered on a global scale, possessing an overall axis of alignment with components that are delineable into recognizable metrics, such as toroidal and poloidal. Nevertheless, cosmic magnetic fields often present a tangled, almost random appearance on the size scale of interest for synchrotron radiation. Figure 1.2 illustrates this situation in

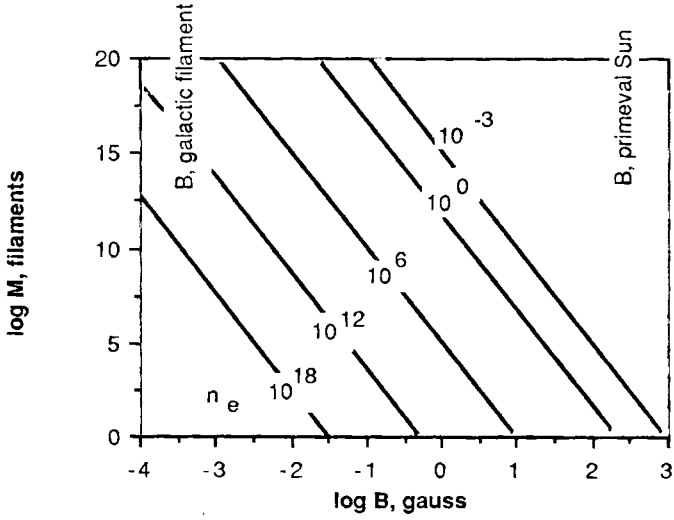

Figure 7.12. Number of filaments of average density n_e cm^{-3} required to produce a blackbody spectrum to 100 GHz versus magnetic field. The graph pertains to mildly relativistic electron temperatures.

a laboratory plasma where current filaments generally flow in a preferred direction but flare, twist, and kink to produce a total magnetic field which, for all practical purposes, is "random."

In the following analyses, a particularly convenient assumption is that the magnetic field lines are essentially uniform on a scale length which is large with respect to the radiating electron gyroradii r_L, but randomly distributed on scales which are small compared to the size of the filament itself.

Previously we considered the case of a single magnetic field orientation $\mathbf{B}_0 = \hat{z}\, B_\ell$. For this case the spectral power radiated by relativistic particles was simply a sum of the different mode polarizations. In a completely random magnetic field, polarization is absent. The spectral power is calculated by averaging the total spectral power for a homogeneous magnetic field Eq.(6.71) over all possible azimuthal and polar (helical-pitch) angles, ϕ and ϑ, respectively.

$$P_\omega(\omega,\gamma) = \frac{1}{4\pi}\int_0^{2\pi} d\phi \int_0^{\pi} P_\omega(\omega, \vartheta, \gamma) \sin\vartheta \, d\vartheta$$

$$= \frac{e^2}{\sqrt{3}\,8\pi^2\varepsilon_0 c}\,\frac{\omega}{\gamma^2}\int_0^{\pi} d\vartheta \sin\vartheta \int_{x/\sin\vartheta}^{\infty} dy\ K_{5/3}(y)$$

$$= \frac{e^2}{\sqrt{3}\,8\pi\,\varepsilon_0 c}\,\frac{\omega}{\gamma^2}\,C\left(\frac{2\,\omega}{3\,\omega_b\gamma^2}\right)\ \mathrm{J\ s^{-1}\ rad^{-1}} \tag{7.93}$$

where $C(x)$ is the Crusius–Schlickeiser function, defined by

$$C(x) = W_{0,4/3}(x)\,W_{0,1/3}(x) - W_{1/2,5/6}(x)\,W_{-1/2,5/6}(x) \tag{7.94}$$

where $W_{\lambda,\mu}(x)$ denotes the Whittaker function. Based of the properties of $W_{\lambda,\mu}(x)$ for small and large arguments [Abramowitz and Stegun 1970], assymptotic expansions of $C(x)$ are

$$C(x) = \begin{cases} a_0 x^{-2/3} & x << 1 \\ x^{-1} e^{-x} & x >> 1 \end{cases} \tag{7.95}$$

where $a_0 = 2^{4/3}\Gamma^2(1/3)/5\pi = 1.151275$. Figure 7.13 is a plot of Eqs.(7.93) and (7.95).

7.6.1 Plasma Effects

The influence of a background plasma on synchrotron emission enters via the refractive index n. Consider, for simplicity, the case of a transverse electromagnetic wave propagating in an isotropic

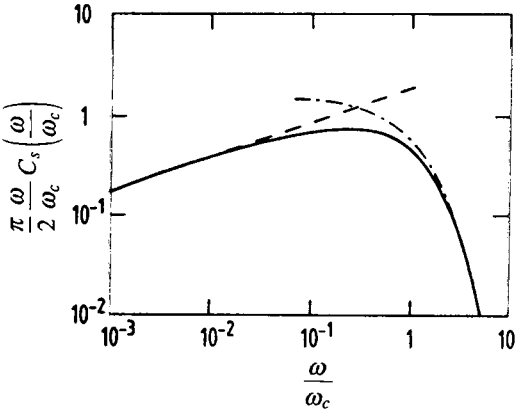

Figure 7.13. Emissivity function as a function of normalized frequency ω/ω_c. The dashed curves show the asymptotic results [Crusius and Schlickeiser 1986].

plasma (Example 7.1), $n^2 = P = 1 - \omega_p^2 / \omega^2$. Since n is less than unity the phase velocity $v_{ph} = \omega / k\, n = c / n$ of the wave is greater than the speed of light. All γ factors in the synchrotron formulae that are due to retardation effects undergo the following transformation:

$$\gamma' = \left(1 - v^2 / v_{ph}^2\right)^{-1/2} = \left(1 - n^2\, v^2 / c^2\right)^{-1/2} \tag{7.96}$$

For relativistic particles $v \approx c$ and Eq.(7.96) becomes

$$\gamma' \approx \gamma / t, \quad t = \left(1 + \gamma^2 \omega_p^2 / \omega^2\right)^{1/2} \tag{7.97}$$

The influence of an isotropic background plasma is manifested by the fact that γ' can be much smaller than the usual Lorentz factor γ. In the plasma Eq.(6.70) has to be changed

$$\omega_c' = \frac{3}{2}\, \omega_\gamma\, \gamma^3\, t^{-3} = \omega_c\, t^{-3} \tag{7.98}$$

Substituting Eq.(7.98) into Eq.(7.93) leads to

$$P_\omega(\gamma) = \frac{e^2}{\sqrt{3}\, 8\, \pi\, \varepsilon_0\, c}\, \frac{\omega}{\gamma^2}\left[1 + \left(\gamma \frac{\omega_p}{\omega}\right)^2\right] C\left\{\frac{2\,\omega}{3\,\omega_b\,\gamma^2}\left[1 + \left(\gamma \frac{\omega_p}{\omega}\right)^2\right]^{3/2}\right\} \quad \mathrm{J\ s^{-1}\ rad^{-1}} \tag{7.99}$$

7.6.2 Monoenergetic Electrons

Consider the case of a monoenergetic distribution of relativistic electrons

$$N(W)\, dW = N(\gamma)\, d\gamma = N_0\, \delta(\gamma - \gamma_0) d\gamma \tag{7.100}$$

Substituting Eqs.(7.99) and (7.100) into Eq.(7.80), we find

$$j_\omega = \int P_\omega(W)\, N(W)\, dW = N_0 \int P_\omega(\gamma)\, \delta(\gamma - \gamma_0)\, d\gamma$$

$$= \frac{N_0\, e^2}{\sqrt{3}\, 8\, \pi\, \varepsilon_0 c}\, \frac{\omega}{\gamma_0^2}\left[1 + \left(\gamma_0 \frac{\omega_p}{\omega}\right)^2\right] C\left\{\frac{2\,\omega}{3\,\omega_b\,\gamma_0^2}\left[1 + \left(\gamma_0 \frac{\omega_p}{\omega}\right)^2\right]^{3/2}\right\} \tag{7.101}$$

or

$$j_\omega = \frac{N_0\, e^2}{\sqrt{3}\, 8\, \pi\, \varepsilon_0 c\, \gamma^2} f\left[1+f^{-2}\right] C\left(\frac{f}{g_0}\left[1+f^{-2}\right]^{3/2}\right) \tag{7.102}$$

where

$$f = \frac{\omega}{\gamma_0\, \omega_p} \tag{7.103}$$

$$g_0 = \frac{3}{2}\left(\frac{\omega_b}{\omega_p}\right)\gamma_0 \tag{7.104}$$

Figure 7.14 illustrates the behavior of the emissivity j_ω versus frequency f for various values of g_0. The emissivity can be characterized according to the magnetic field/plasma density parameter g_0. For most cosmic plasma $\omega_b \leq \omega_p$ so that $g_0 >> 1$ corresponds to highly relativistic of electrons $\gamma_0 >> 1$. The spectra of Figure 7.14 for large frequencies is typical of that generated by relativistic electrons in the absence of plasma effects (c.f., Figure 7.13). This vacuum behavior extends down to a lower frequency $f \approx g_0^{-1/2}$. The logarithmic bandwidth of j_ω is [Crusius 1988]

$$\Delta \log f \cong 1.5 \log g_0 \tag{7.105}$$

The larger g_0, the larger the logarithmic bandwidth with its characteristic anisotropy around $f = 1$.

When $g_0 < 1$ $(\omega_p > \omega_b \gamma_0)$, Figure 7.14 shows an exponential surpression for all frequencies when compared to the case of $g_0 >> 1$.

The parameter g_0 may also be written as

$$g_0 = \frac{\gamma_0}{\gamma_R} \tag{7.106}$$

where

$$\gamma_R = \frac{2}{3}\frac{\omega_p}{\omega_b} = \frac{2.1 \times 10^{-10}\sqrt{n_e\,(\mathrm{m}^{-3})}}{B\,(\mathrm{T})} \tag{7.107}$$

is called the Razin–Lorentz factor in a random magnetic field.

7.7 Anisotropic Distribution of Velocities

Only the energy conservation equation was used in the derivation of Eq.(7.77) to Eq.(7.83). However, for an anisotropic distribution function, momentum conservation equations are also needed.

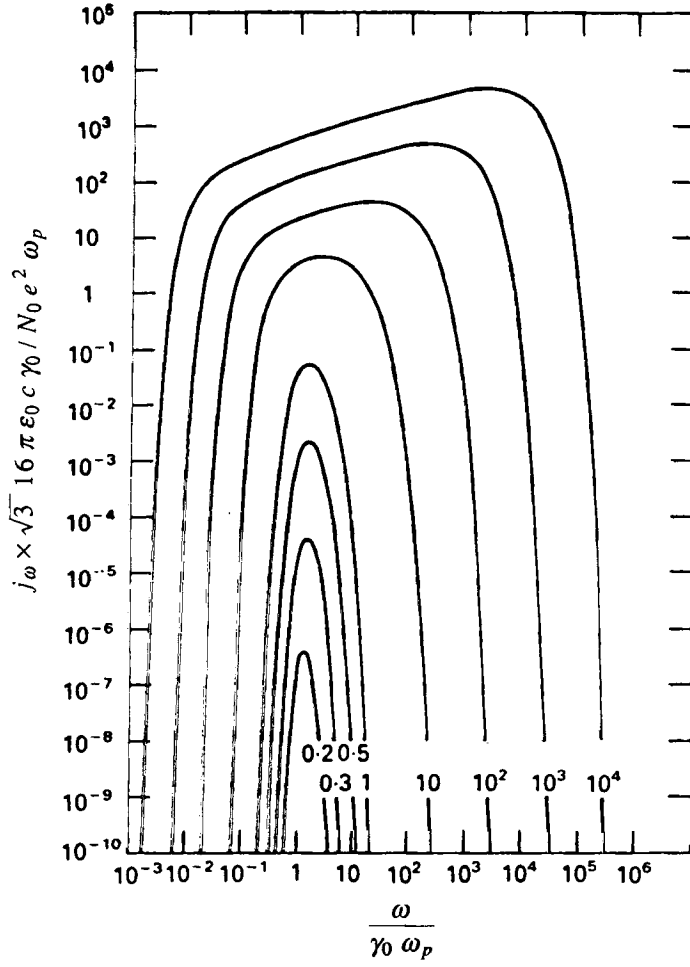

Figure 7.14. Emission coefficient j_ω as a function of the normalized frequency f for $g_0 = 0.2, 0.3, 0.5, 1, 10, 10^2, 10^3$, and 10^4 [Crusius 1988].

Let $f(p_\parallel, p_\perp)$ be the distribution of particle momenta where $p_\parallel$ and $p_\perp$ are the components of $\mathbf{p}$ parallel and perpendicular to $\mathbf{B}_0$, respectively. We assume for simplicity that $f(p_\parallel, p_\perp)$ is symmetrical about the $\mathbf{B}_0$ direction, namely, that there is no dependence of $f(p_\parallel, p_\perp)$ on azimuthal angle ϕ.

Again expanding $f(p_\parallel, p_\perp)$ in a Taylor series, we obtain

$$f(p_{\parallel}', p_{\perp}') = f(p_{\parallel}, p_{\perp}) + \frac{\partial f}{\partial p_{\parallel}} \Delta p_{\parallel} + \frac{\partial f}{\partial p_{\perp}} \Delta p_{\perp} \tag{7.108}$$

The determination of $\Delta p_{\parallel}$, $\Delta p_{\perp}$ requires use of Eq.(7.75) and the momentum conservation equation for $p_{\parallel}$

$$p_{\parallel}' - p_{\parallel} = n(\theta) \cos\theta \frac{\hbar \omega}{c} \tag{7.109}$$

The parameters $\Delta p_{\parallel}$, $\Delta p_{\perp}$ are obtained from the conservation equations Eq.(7.108) and Eq.(7.109) with the result

$$\Delta p_{\parallel} = n(\theta) \cos\theta \frac{\hbar \omega}{c}$$

$$p_{\perp} \Delta p_{\perp} = \frac{W \hbar \omega}{c^2} - p_{\parallel} n(\theta) \cos\theta \frac{\hbar \omega}{c} \tag{7.110}$$

Using Eqs.(7.108) and (7.110) and the fact that $d^3 p' \rightarrow d p = 2 \pi p_{\perp} dp_{\perp} dp_{\parallel}$, the emission and absorption coefficients Eq.(6.85b) and Eq.(7.68) reduce to

$$i_{\omega} = \int \int P_{\omega}(p_{\parallel}, p_{\perp}) f(p_{\parallel}, p_{\perp}) 2 \pi p_{\perp} dp_{\perp} dp_{\parallel} \tag{7.111}$$

$$\alpha_{\omega} = -\frac{8 \pi^3 c^2}{n^2 \omega^2} \int \int P_{\omega}(p_{\parallel}, p_{\perp}) \times \left[\frac{W}{c^2} \frac{\partial f}{\partial p_{\perp}} - n(\theta) \cos\theta \left(\frac{p_{\parallel}}{c} \frac{\partial f}{\partial p_{\parallel}} - \frac{p_{\perp}}{c} \frac{\partial f}{\partial p_{\perp}} \right) \right] 2\pi p_{\perp} dp_{\perp} dp_{\parallel} \tag{7.112}$$

It should be noted that Eq.(7.112) contains both the ray refractive index n and the wave index $n(\theta)$. When f is isotropic Eq.(7.111) and Eq.(7.112) reduce to Eq.(7.77) and Eq.(7.78), respectively.

Equation (7.111) has found application in the study of radio bursts of synchrotron radiation at decameter wavelengths from Jupiter for the special case $n \rightarrow 1$, $\theta = \pi/2$ [Hirshfield and Bekefi 1963].

Notes

[1] The discovery that radio waves could "follow" the curvature of the earth caused O. Heaviside and A. Kennelly to simultaneously suggest, in 1901, the existence of a plasma ionosphere which would cause the waves to reflect or "skip" between the earth and this layer.

[2] The operator d/ds represents $\hat{s} \cdot \nabla$ where $\hat{s}$ is a unit vector along the ray direction s.